Theoretical Studies of Ziegler–Natta Catalysis: Structural Variations and Tacticity Control

Erik P. Bierwagen,† John E. Bercaw,‡ and W. A. Goddard, III*,†

Contribution from the Materials and Molecular Simulations Center, Beckman Institute (139-74), and Arnold and Mabel Beckman Laboratories of Chemical Synthesis, Division of Chemistry and Chemical Engineering (Contribution No. 8821), California Institute of Technology, Pasadena, California 91125

Received June 30, 1992. Revised Manuscript Received November 22, 1993•

Abstract: Models for the likely active catalysts in homogeneous Ziegler–Natta systems have been studied using *ab initio* quantum chemical methods. We investigated the geometries of the isoelectronic model complexes, X_2M–R where X = Cl or Cp = (η^5-C_5H_5); where M = Sc and Ti^+ (and also Ti); and where R = H, CH_3, or SiH_3. The general trend is that the M = Sc compounds strongly prefer a planar configuration, whereas the M = Ti^+ cases generally prefer pyramidal geometries. This difference in geometry can be related to the differing ground-state electronic configurations for the metals: Sc is $(4s)^2(3d)^1$, whereas Ti^+ is $(4s)^1(3d)^2$. The nonplanar geometry for $[Cp_2Ti–R]^+$ suggests an explanation for the origin of stereospecificity in the syndiotactic polymerization by unsymmetric metallocene catalysts. These results suggest that {(η^5-C_5H_4)CMe_2(η^5–fluorenyl)}Sc–R would *not* catalyze syndiotactic polymerization under these conditions.

I. Introduction

Following its discovery[1] in the mid 1950s, Ziegler–Natta polymerization of olefins has evolved into a major industrial process, producing tens of billions of pounds of polyethylene and polypropylene per year. Despite its tremendous importance, the basic polymerization mechanism remains controversial. Recent advances in understanding the structure of the active catalyst have been facilitated by the discovery of relatively well-defined Ziegler–Natta α-olefin polymerization systems: (1) two-component catalysts consisting of group 4 metallocene dihalides and a large excess of methylalumoxane cocatalyst,[2,3] (2) simpler two component systems based on group 4 metallocene dialkyls with a stoichiometric (or near stoichiometric) amount of activator such as $[C_6H_5(CH_3)_2NH^+][B(C_6F_5)_4^-]$,[4] $[(C_6H_5)_3C^+][B(C_6F_5)_4^-]$,[5] or $B(C_6F_5)_3$,[6] and (3) single component catalysts such as Lewis base–adducts of cationic group 4 metallocene alkyls[7] or the isoelectronic neutral group 3 or lanthanide metallocene hydrides or alkyls.[8,9] There is a growing consensus that these systems all have a common catalytically active species, the 14-electron, bis(cyclopentadienyl)metal alkyl cation, $[Cp_2M–R]^+$ (M = group 4 metal) or Cp_2M–R (M = group 3 or lanthanide metal). By suitable substitution of the metallocene structure, variations in polymer microstructure may be introduced. For example, with chiral catalysts or catalyst precursors, highly isotactic polypropylene has been obtained. Ewen[10] described the syndiospecific polymerization of propylene using the achiral, asymmetric catalyst precursors {(η^5-C_5H_4)CMe_2(η^5-fluorenyl)}-MR_2 (M = Zr, Hf; R = Cl, CH_3) in combination with methylalumoxane (eq 1).

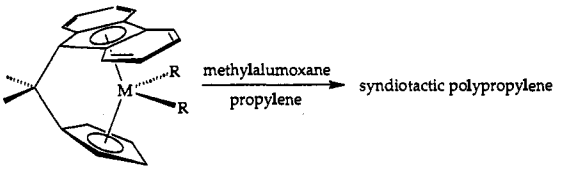

(1)

{Me_2C(Fl)Cp}MX_2

(M = Zr, Hf; R = Cl, CH_3)

Whereas the features responsible for tacticity control are not fully understood at present, an attractive proposal for the syndiospecificity is shown in Scheme 1.

An essential feature is the requirement that olefin coordination occurs as shown, that is, with the propylene methyl substituent directed toward the smaller cyclopentadienyl ligand[11] *and olefin*

* To whom correspondence should be addressed.
† Materials and Molecular Simulations Center.
‡ Arnold and Mabel Beckman Laboratories of Chemical Synthesis.
• Abstract published in *Advance ACS Abstracts,* January 15, 1994.

(1) (a) Ziegler, K.; Holzkamp, E.; Breil, H.; Martin, H. *Angew. Chem.* **1955**, *67*, 541. (b) Natta, G. *Macromol. Chem.* **1955**, *16*, 213.

(2) (a) Kaminsky, W.; Kulper, K.; Brintzinger, H. H.; Wild, F. R. W. P. *Angew. Chem., Int. Ed. Engl.* **1985**, *24*, 507. (b) Ewen, J. A. *J. Am. Chem. Soc.* **1984**, *106*, 6355. (c) Rieger, B.; Mu, X.; Mallin, D. T.; Rausch, M. D.; Chien, J. C. W. *Macromolecules* **1990**, *23*, 3559. (d) Erker, G.; Nolte, R.; Aul, R.; Wilker, S.; Kruger, C.; Noe, R. *J. Am. Chem. Soc.* **1991**, *113*, 7594. (e) Chien, J. C. W.; Llinas, G. H.; Rausch, M. D.; Lin, G. Y.; Winter, H. H. *J. Am. Chem. Soc.* **1991**, *113*, 8569. (f) Soga, K.; Shiono, T.; Takemura, S.; Kaminsky, W. *Makromol. Chem., Rapid Commun.* **1987**, *8*, 305. (g) Ewen, J. A.; Haspeslagh, L.; Atwood, J. L.; Zhang, H. *J. Am. Chem. Soc.* **1987**, *109*, 6544. (h) Ewen, J. A.; Elder, M. J.; Jones, R. L.; Haspeslagh, L.; Atwood, J. L.; Bott, S. G.; Robinson, K. *Makromol. Chem., Macromol. Symp.* **1991**, *48/49*, 253.

(3) Sinn, H.; Kaminsky, W.; Vollmer, H. J.; Woldt, R. *Angew. Chem., Int. Ed. Engl.* **1980**, *19*, 390.

(4) (a) Hlatky, G. G.; Turner, H. W.; Eckman, R. R. *J. Am. Chem. Soc.* **1989**, *111*, 2728. (b) Turner, H. W. European Patent Application 277004, 1988.

(5) (a) Ewen, J. A.; Elder, M. J. European Patent Application 426,638, 1991. (b) Chien, J. C. W.; Tsai, W.-M.; Rausch, M. D. *J. Am. Chem. Soc.* **1991**, *113*, 8570.

(6) (a) Ewen, J. A.; Elder, M. J. European Patent Application 427,697, 1991. (b) Yang, X.; Stern, C. L.; Marks, T. J. *J. Am. Chem. Soc.* **1991**, *113*, 3623.

(7) (a) Jordan, R. F.; Bradley, P.; Baenziger, N. C.; LaPointe, R. E. *J. Am. Chem. Soc.* **1990**, *112*, 1289. (b) Jordan, R. F.; LaPointe, R. E.; Bradley, P. K.; Baenziger, N. *Organometallics* **1989**, *8*, 2892. (c) Eshuis, J. J. W.; Tan, Y. Y.; Meetsma, A.; Teuben, J. H.; Renkema, J.; Evens, G. G. *Organometallics* **1992**, *11*, 362.

(8) (a) Watson, P. L. *J. Am. Chem. Soc.* **1982**, *104*, 337. (b) Burger, B. J.; Thompson, M. E.; Cotter, W. D.; Bercaw, J. E. *J. Am. Chem. Soc.* **1990**, *112*, 1566. (c) Jeske, G.; Lauke, H.; Mauermann, H.; Sweptson, P. N.; Schumann, H.; Marks, T. J. *J. Am. Chem. Soc.* **1985**, *107*, 8091.

(9) Coughlin, E. B.; Bercaw, J. E. *J. Am. Chem. Soc.* **1992**, *114*, 7606.

(10) Ewen, J. A.; Jones, R. L.; Razavi, A.; Ferrara, J. D. *J. Am. Chem. Soc.* **1988**, *110*, 6255.

(11) Whether the methyl is directed toward the big or small ligand has not yet been solved conclusively, although results from Ewen *et al.* (Ewen, J. A.; Elder, M. J. *Makromol. Chem., Macromol. Symp.* **1993**, *66*, 179) and Cavallo et al. (Cavallo, L.; Guerra, G.; Vacatello, M.; Corradini, P. *Macromolecules* **1991**, *24*, 1784) suggest that the methyl group is pointed toward the large ligand; as long as the methyl is consistently directed toward the same ligand, the size of the ligand does not affect the qualitative scheme described.

0002-7863/94/1516-1481$04.50/0

Scheme 1

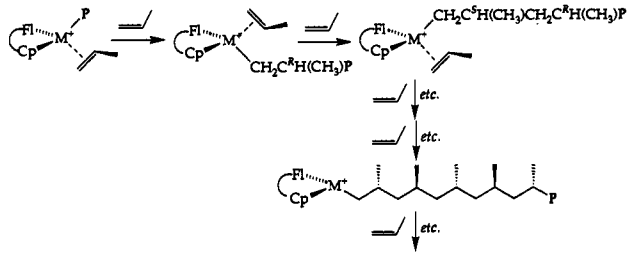

insertion regularly alternating from side to side of the equatorial plane of the metallocene cation. The origin of this alternation has been the subject of considerable interest.[12] One possibility is that there is an inherent preference for the growing polymer chain to reside at a lateral site (structure B).

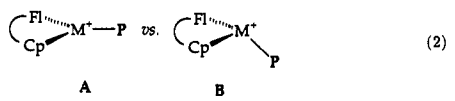

(2)

Combined with the accepted four-center transition state,[13] such a preference would lead to the polymer's regularly alternating from side to side of the equatorial plane:

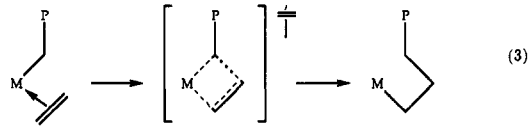

(3)

Moreover, if there exists a preference for the growing polymer chain to reside at a lateral rather than central equatorial position, it would be of further interest to establish the barrier for the nearly degenerate[14] "swing" from side to side (eq 4).

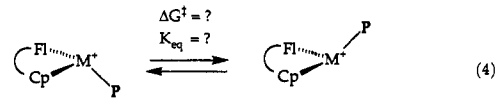

(4)

In order to address these issues we report here studies on:

(5)

where (i) M = Sc, Ti^+, Ti; (ii) X = Cl and Cp; and (iii) R = H, CH_3, and SiH_3. We find in all cases that X_2MR prefers a *planar geometry* (**A**) for the group 3 and group 4 *neutral species*. However, the group 4 cations have a strong bias (by up to 15 kcal/mol) toward nonplanar geometries (**B**). We conclude that (1) the preference of nonplanar geometries by the group 4 cations explains the syndiotacticity observed by providing a rationale for the side-to-side alternation of Scheme 1, and (2) homogeneous catalysts based on group 3 and group 4 neutrals will not exhibit such stereospecificity.

II. Results

A. Calculational Details. All calculations used *ab initio* quantum chemical methods with the generalized valence bond (GVB) method[15] to include electron correlation between the metal (M) and alkyl or hydrogen ligands (R) and effective core potentials[16] (ECP) to replace the inner core electrons of Ti, Sc, Cl, and Si. Further details are in the Calculation Details section.

Table 1. Geometries of L_2MR, Based on GVB(1/2) Calculations[a,k]

species	*R*-(M–R)	*R*-(M–X)	*θ*-(XMX)	*ω*-(plane–R)[b]	*θ*-(RMX)[c]
Cl_2ScH	1.74	2.36	139.1	0.0	110.4
Cl_2TiH^+	1.69	2.18	120.5	84.4	92.6
Cl_2TiH	1.68	2.32	147.8	0.0	106.1
$Cl_2Sc(CH_3)$	2.15[d]	2.40	141.9	0.0	109.1
$Cl_2Sc(SiH_3)$	2.79[e]	2.39	151.0	0.0	104.0
$Cl_2Ti(CH_3)^+$	1.99[f]	2.20	115.5	64.5	99.4
$Cl_2Ti(SiH_3)^+$	2.89[g]	2.23	126.3	89.7	90.4
Cp_2ScH	1.82	(2.17)	(143.0)	0.0	(108.5)
$Cp_2Sc(CH_3)$	2.28[h]	(2.17)	(143.0)	0.0	(108.5)
Cp_2TiH^+	1.73	(2.07)	(132.6)	65.0	99.8
$Cp_2Ti(CH_3)^+$	2.20, 2.26[i,j]	(2.07)	(132.6, 118.0)[i]	0.0	113.7

[a] In the Cp systems, X refers to the Cp centroid. Fixed values are in parentheses. The CC bond lengths of Cp were fixed at 1.40 Å and the CH bond lengths at 1.08 Å. [b] The plane is defined by the metal and the chlorines or Cp centroids. The angle is relative to the axis away from X. [c] θ_{RMX} is determined by θ_{XMX} and ω. [d] R_{CH} = 1.09, θ_{HCH} = 109, optimized. [e] R_{SiH} = 1.48, θ_{HSiH} = 111°, optimized. [f] R_{CH} = 1.09, θ_{HCH} = 114°, optimized. [g] R_{SiH} = 1.46, θ_{HSiH} = 117°, optimized. [h] R_{CH} = 1.09, θ_{HCH} = 109.5, fixed. [i] $R_{(Ti-CH_3)}$ = 2.20, θ_{XMX} = 132.6; $R_{(Ti-CH_3)}$ = 2.26, θ_{XMX} = 118.0. [j] R_{CH} = 1.09, θ_{HCH} = 114°, fixed. [k] Distances (*R*) in Å, angle (*θ*) in deg.

B. Cl_2ScH, Cl_2TiH^+. Since Cl_2ScH and Cl_2TiH^+ are isoelectronic, these two complexes might be expected to have similar geometries, yet they are quite different. Cl_2ScH has a planar geometry (and requires a 1.53 kcal/mol energy increase to move H out of the plane by 50°), whereas Cl_2TiH^+ has a nonplanar geometry with the hydrogen 84° out of the plane (with a planar structure 12.8 kcal/mol higher in energy) (see Table 1 for the complete geometries). Others[17] have also found noncoplanar structures for Cl_2MR^+, where M is a group 4 metal. However, no convincing explanation has been put forward as to why this occurs. By electrostatic and steric arguments it is counterintuitive: all of the ligands, which are formally negatively charged, are crowded near to each other. On the other hand, Lauher and Hoffmann,[18] in their study of Cp_2TiH^+, predicted that all formally d^0 metal systems would demonstrate this noncoplanar effect, since the LUMO for Cp_2M is directed to the side of the wedge, rather than towards the center. In contrast to this analysis, we find that the scandium systems are planar.

Our *ab initio* studies show that these tendencies can be best understood in terms of the electronic configurations of the metal ground state: Sc is $(4s)^2(3d)^1(^2D)$, whereas isoelectronic Ti^+ is $(4s)^1(3d)^2(^4F)$ (see Table 2); to reduce electronic repulsion between the two d electrons of Ti^+, one occupied d orbital lies in a plane (e.g., d_{xy} or $d_{x^2-y^2}$), while the other d orbital is perpendicular to this plane (e.g., d_{z^2}). Generally it is found[19] that electronegative ligands bond to a transition-metal bond preferentially via 4s over 3d orbitals. Thus bonding two Cl's or Cp's to Sc uses the two 4s-like orbitals (as 4s + 4pz and 4s-4pz hybrids)

(12) It has been argued that a second olefin assists the insertion and forces the alternating migratory insertion: Ystenes, M. *J. Catal.* **1991**, *129*, 383; however, most studies have established a first-order rate dependence for olefin. Watson, P. L. *J. Am. Chem. Soc.* **1982**, *104*, 337. Chien, J. C. *J. Am. Chem. Soc.* **1959**, *81*, 86.

(13) (a) Cossee, P. *Tetrahedron Lett.* **1960**, *17*, 12. (b) Cossee, P. *J. Catal.* **1964**, *3*, 80. (c) Arlman, E. J.; Cossee, P. *J. Catal.* **1964**, *3*, 99. (d) Arlman, E. J. *J. Catal.* **1966**, *5*, 178.

(14) In propylene polymerization the two lateral sites are diastereotopic due to the chirality of the *β* carbon center.

(15) (a) Bobrowicz, F. W.; Goddard, W. A., III *Methods of Electronic Structure Theory*; Schaefer, H. F., III, Ed.; Plenum Publishing Corp.: 1977. (b) Goddard, W. A., III; Ladner, R. C. *J. Am. Chem. Soc.* **1971**, *93*, 6750. (c) Ladner, R. C.; Goddard, W. A., III *J. Chem. Phys.* **1969**, *51*, 1073. (d) Hunt, W. J.; Hay, P. J.; Goddard, W. A., III *J. Chem. Phys.* **1972**, *57*, 738.

(16) (a) Melius, C. F.; Goddard, W. A., III *Phys. Rev. A* **1974**, *10*, 1528. (b) Redondo, A.; Goddard, W. A., III; McGill, T. C. *Phys. Rev. B* **1977**, *15*, 5038. (c) Rappé, A. K.; Smedley, T. A.; Goddard, W. A., III *J. Chem. Phys.* **1981**, *85*, 1662. (d) Hay, P. J.; Wadt, W. R. *J. Chem. Phys.* **1985**, *82*, 299. (e) Hurley, M. M.; Pacios, L. F.; Christiansen, P. A.; Ross, R. B.; Ermler, W. C. *J. Chem. Phys.* **1986**, *84*, 6840.

(17) (a) Jolly, C. A.; Marynick, D. S. *J. Am. Chem. Soc.* **1989**, *111*, 7968. (b) Kawamura-Kuribayashi, H.; Koga, N.; Morokuma, K. *J. Am. Chem. Soc.* **1992**, *114*, 2359. (c) Castonguay, L. A.; Rappé, A. K. *J. Am. Chem. Soc.* **1992**, *114*, 5832. (d) Jolly, C. A.; Marynick, D. S. *Inorg. Chem.* **1989**, *28*, 2893.

(18) Lauher, J. W.; Hoffmann, R. *J. Am. Chem. Soc.* **1976**, *98*, 1729.

Table 2. Atomic State Splittings[e]

atom/ion	ground state	excited state	excitation energy theory[a]	excitation energy experiment[b]
Sc[c]	$^2D(s^2d^1)$	$^4F(s^1d^2)$	1.09	1.43
Ti^+ [d]	$^4F(s^1d^2)$	$^2D(s^2d^1)$	−4.26	−3.08
Ti[d]	$^3F(s^2d^2)$	$^5F(s^1d^3)$	0.98	0.81

[a] All s^2 states are calculated using the GVB(1/2) wave function. [b] See ref 21. [c] Basis sets and ECPs from ref 16d. [d] Basis sets listed in the appendix, ECPs from ref 16e. [e] The excitation energy is for $\Delta E = E(s^1d^n) - E(s^2d^{n-1})$.

leaving a single electron in a d orbital for bonding to an H or alkyl. However for titanium there is only one s electron and the Cl's or Cp's bond via sd hybrids; again the H or alkyl bonds to the remaining d electron. In this case (Ti^+) the M–X bonds uses d_{xy}-s hybrids and the M–R bond uses d_{z^2}. This bonding scheme is consistent with the calculations and leads naturally to the observed geometries for both Sc and Ti^+.

Our general paradigm for understanding structure and reactivity of complex molecules is the *valence bond fragment* (VBF) analysis in which (i) the molecule is broken into fragments, (ii) the orbital character of the fragments is analyzed, and then (iii) the molecule is reassembled based on the orbital character of the fragments. VBF analysis closely resembles the orbitals obtained from GVB calculations, and indeed the confidence in using VBF analysis is based on many previous GVB studies.[19,20] In VBF analysis, the wave functions are optimal for the fragment but may not be optimal for bonding in the parent molecule. We present here two different VBF analyses of the Cl_2MH systems to help understand why they exhibit such different structural characteristics. We must emphasize that such VBF analyses are meant to guide the reasoning. For molecules having a low-lying excited state with different character, the combined molecule might resemble the excited state if this provides stronger bonding. The real test is the GVB wave function for the complete molecule.

1. ClMH. We studied the ClMH fragment to determine the character for an optimal M–H bond. At the GVB(1/2) level (correlating the M–H bond) the Cl–Sc–H angle is 180°, while the Cl–Ti–H angle is 100°. This difference in geometry arises from the difference in atomic configurations of $Sc(s^2d^1)$ and $Ti^+(s^1d^2)$.

In ClScH each ligand bonds to the metal via metal sp hybrids (as usual for s^2 states), leaving a singly-occupied d orbital in the plane bisecting the Cl–Sc–H angle. The M–H bond pair has 1.24 of the two electrons transferred to the H and has Sc hybridization of 19% d and 81% sp; the M–Cl bond has 1.79 of the two electrons transferred to Cl with 37% d and 63% sp on Sc. The unpaired orbital is d_{xy} (taking the molecular axis as z). The net population on the Sc is 61% d and 39% sp (see Table 3).

In contrast, for $ClTiH^+$ the M–H bond involves only 0.85 e transferred to H and the Ti^+ portion is 79% d and 21% sp. Here the M–Cl bond involves 1.50 e transferred to Cl and has sd (55% sp and 45% d) metal hybrid character, with a net Ti^+ population of 79% d, 21% sp. The singly-occupied orbital is a d_{z^2}-like orbital nearly perpendicular to both the M–H and M–Cl bonds (taken as the xy plane). $ClTiH^+$ is bent in order to maintain orthogonality between the metal $d\sigma$ orbitals used in the M–H and M–Cl bonds. Thus, the s^1d^2 state imparts an electronic influence on the geometry of the $ClTiH^+$ species due to the metal d component of the metal ligand bonds. This explains why the best structure of $ClTiH^+$ is bent, with the singly-occupied orbital perpendicular to the ClTiH plane.

(19) (a) Steigerwald, M. L.; Goddard, W. A., III *J. Am. Chem. Soc.* **1984**, *106*, 308. (b) Steigerwald, M. L.; Goddard, W. A., III *J. Am. Chem. Soc.* **1985**, *107*, 5027. (c) Rappé, A. K.; Goddard, W. A., III *J. Am. Chem. Soc.* **1980**, *102*, 5114. (d) Rappé, A. K.; Goddard, W. A., III *Potential Energy Surfaces and Dynamics Calculations*; Truhlar, D. G., Ed.; Plenum Press: New York, 1981; pp 661–684. (e) Rappé, A. K.; Goddard, W. A., III *J. Am. Chem. Soc.* **1982**, *104*, 297.

(20) Low, J. J.; Goddard, W. A., III *J. Am. Chem. Soc.* **1986**, *108*, 6115.

Table 3. Metal Character of Metal–Ligand Bonds in ClMH for θ = 180° and θ = 100° [a]

	optimum bond angle	M character of M–H bond, θ = 180° %s	%p	%d	charge	θ = 100° %s	%p	%d	charge
ClScH	180	43	37	20	0.75	48	22	30	0.82
$ClTiH^+$	100	7	19	74	1.09	13	8	79	1.15

[a] Results are based on GVB(2/4) wave functions, and analyses are based on Mulliken populations of each GVB pair.

2. Cl_2M. Since Cl is much more electronegative than the metal, there is some charge transfer from M to Cl. This charge transfer is primarily out of the M s orbital since it is much more easily ionized. Thus, the chlorines preferentially bond to the metal via metal s orbitals (or polarized sp hybrids) rather than d orbitals. By polarizing the 4s pair with 4p orbitals, scandium can form two bonds that are of predominantly metal-s character, leaving a singly-occupied d-orbital that prefers to be in the plane bisecting the Cl–Sc–Cl angle. The two Cl–M bonds prefer to be parallel (180° bond angle), because of hybridization and minimization of the electrostatic repulsion between the chlorines. Indeed we find the Cl–Sc–Cl angle of $ScCl_2^•$ to be 180°. However, the energy to bond at an angle of 126° is only 5.69 kcal/mol higher.

The titanium case is much different. Ti^+ has only one valence s electron, so that the two metal–chlorine bonds must incorporate some metal sd character. If the s and d orbitals had the same radial character, then mixing of 4s and $3d_{xy}$ (or $d_{x^2-y^2}$) would lead to 90° bonds. We find that the $TiCl_2^{•+}$ fragment has an optimum angle of 126° with an energy 7.24 kcal/mol below that of the linear geometry. In addition to the radial mismatch, this increase from 90° is partially due to Cl–Cl electrostatic repulsion, causing the metal to mix in some $d^3(^4F)$ character (the s^1d^2 to d^3 excitation energy is only 2.78 kcal/mol).[21] At the optimum angle of 126° (which results from s^1d^2), the remaining singly-occupied orbital has a pure d character and lies in the symmetry plane bisecting the ClTiCl angle.

The singly-occupied orbitals for $ScCl_2^•$ and $TiCl_2^{•+}$ are plotted in Figure 1, where we see that they are nearly identical. In addition we show in Figure 1 the orbitals of bent $ScCl_2^•$ (θ = 126°). Taking the symmetry axis of the bent molecule as z and the plane of the molecule as yz, the unpaired orbital has $d_{z^2-x^2}$ character.

3. Cl_2MH. The optimum geometry for Cl_2ScH (Table 1) leads to a ClScCl angle that drops from 180° to 140° as the H bonds to the d_{z^2} orbital in the ClScCl plane, leading to a planar molecule. On the other hand, with Cl_2TiH^+ the H bonds to the x^2 lobe of the $d_{z^2-x^2}$ orbital, leading to an angle of 84° (measured from the axis away from chlorines) and the Cl–Ti–Cl angle decreases slightly from 126° to 120°, reflecting increased d character in the Ti–Cl bonds accompanying the incorporation of s character in the M–H bond. Thus the geometries are explained by the difference in atomic character $Sc(s^2d^1)$ versus $Ti^+(s^1d^2)$.

We also studied the neutral $Cl_2TiH^•$. Since Ti has an $s^2d^2(^3F)$ ground state, the above arguments suggest that the *neutral* group 4 compounds would be planar. Here we expect the metal character of the metal–chlorine bonds to be primarily of s character (as for the group 3 cases) and for the metal–hydrogen bond to have no directionality imposed upon it. Indeed, as shown in Table 1, the geometry of this complex is planar.

C. Analysis of the Metal Character in Cl_2MH Bonds. The GVB orbitals for various systems are shown in Figure 2. To obtain quantitative measurements of bond character, we resolved each GVB bond pair in terms of the atomic character on the metal and the charge transfer. The results are listed in Table 4. The metal character of the bonds for the Sc, Ti^+, and Ti systems

(21) Moore, C. E. *Atomic Energy Levels*; Vol. I, NBS Ref. Data Series, NBS 35, U.S. Government Printing Office, Washington, DC, 1971; pp 259–290.

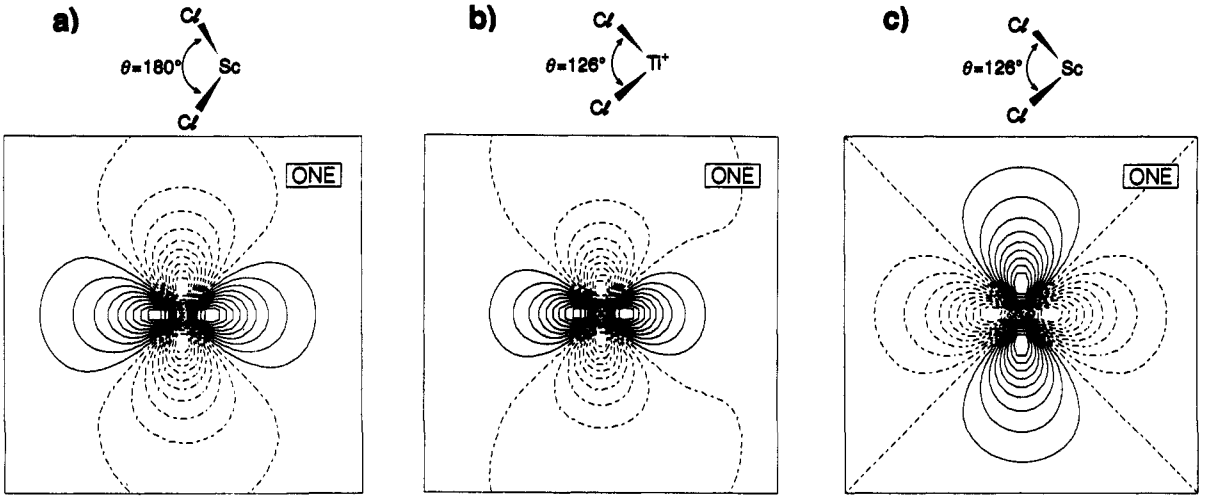

Figure 1. Singly occupied orbital for Cl_2M^*: (a) Cl_2Sc, $\theta = 180°$, (b) Cl_2Ti^+, $\theta = 126°$, and (c) Cl_2Sc, $\theta = 126°$.

Table 4. Metal Character of Metal–Ligand Bonds in Cl_2MH[c]

	total charge			MCl bond				MR bond			
species	M	X	R	M charge	%s	%p	%d	M charge	%s	%p	%d
$ScCl_2$	+0.86	−0.43		0.28	32	30	38				
ClScH	+0.73	−0.48	−0.24	0.21	25	38	37	0.75	43	37	20
Cl_2ScH	+0.87	−0.37	−0.13	0.33	24	33	44	0.93	19	18	63
$Cl_2Sc(CH_3)$	+0.97	−0.38	−0.20	0.31	26	34	40	0.80	13	9	78
$Cl_2Sc(SiH_3)$	+0.59	−0.38	+0.16	0.28	25	33	42	1.17	19	13	68
Cp_2ScH	+0.16	−0.03	−0.13					0.94	20	20	60
$Cp_2Sc(CH_3)$	+0.74	−0.19	−0.35					0.66	14	17	69
$TiCl_2^+$	+1.12	−0.06		0.65	19	20	61				
$ClTiH^+$	+1.03	−0.14	+0.11	0.49	32	32	46	1.15	13	8	79
Cl_2TiH^+	+0.78	+0.01	+0.21	0.64	20	17	63	1.21	11	5	84
Cl_2TiH	+0.70	−0.32	−0.06	0.34	26	35	39	1.00	16	12	72
$Cl_2Ti(SiH_3)^+$	+0.63	−0.10	+0.57	0.59	21	23	56	1.57	10	7	83
$Cl_2Ti(CH_3)$	+0.80	−0.04	+0.16	0.63	20	20	60	1.16	6	3	91
Cp_2TiH^+	+0.41	+0.22	+0.03					1.08	5	11	84
$Cp_2Ti(CH_3)^+$ [a]	+0.48	+0.21	+0.10					1.09	3	7	90
$Cp_2Ti(CH_3)^+$ [b]	+0.53	+0.19	+0.09					1.08	3	7	90

[a] θ(CpTiCp) = 132.6. [b] θ(CpTiCp) = 118.0. [c] Results are based on GVB(2/4) wave functions for MCl_2 systems, GVB(3/6) for Cl_2MH systems, and GVB(1/2) for Cp_2MH systems at the optimum geometries. Analyses are based on Mulliken populations of each GVB bond pair containing two electrons.

differ significantly. In the cases of $Sc(s^2d^1)$ and $Ti(s^2d^2)$, the sp contribution is much larger than for Ti^+. This shows that the ground-state configuration of the metals does indeed influence metal–ligand bonding.

D. Cl_2ScR, Cl_2TiR^+. The hydride systems illustrate the nature of the metal–ligand bonds; however, for Ziegler–Natta catalysis we need to understand the steric and electrostatic demands of the growing polymer chain. Thus we next calculated the geometries of Cl_2MR for R = CH_3, SiH_3 with M = Sc and Ti^+. As shown in Table 1, $Cl_2Ti(CH_3)^+$ is nonplanar (64.5° out of the plane, with a planar structure 9.55 kcal/mol higher in energy), whereas $Cl_2Sc(CH_3)$ is planar (requiring a 1.30 kcal/mol energy increase to move 50° out of the plane). The nonplanar bias of $Cl_2Ti(CH_3)^+$ is less pronounced than for Cl_2TiH^+ (which was 84.4° with a 12.8 kcal/mol barrier to planarity). The origin of this difference is probably electrostatic. The carbon carries a negative charge, leading to a repulsion between the chlorines and the methyl, whereas the hydrogen carries a positive charge, leading to attraction. To test this idea we replaced the methyl group by a silyl group. The silicon has a positive charge and should be more similar to H. Indeed, we find a nonplanar geometry with a 89.7° angle for SiH_3 (compared with 84.4° for H and 65° for CH_3).

E. Cp_2MR. The most realistic models for Ziegler–Natta catalysts use Cp ligands, which mimic the interactions between the polymer chain and the ancillary ligands in the catalysts. The results for both the hydride and methyl complexes are in Tables 1 and 5. We expected and found that in both Cp_2ScH and $Cp_2Sc(CH_3)$ the unique ligands are coplanar with the Cp centroids and the metal. The energy to bend the MR bond out of the plane by 50° is 5.0 and 15.9 kcal/mol, respectively. This indicates a geometric factor (steric plus electronic) of about 11 kcal/mol *against* pyramidal for H going to CH_3. For Cp_2TiH^+, we find that H swings out of the plane described by the Cp centroids and titanium; however, the out-of-plane angle decreases from the 84° in the chloride case to 65° in the Cp case. The energy required to become planar decreases from 12.8 kcal/mol for Cl to 5.2 kcal/mol for Cp, indicating an increased steric factor against pyramidal H of 7.6 kcal/mol for Cl to Cp. Such differences are expected from the difference in size between Cl and Cp. For the chloride systems, the energy as a function of angle out of the plane is plotted in Figure 3, while Figure 4 contains the energy as a function of angle for the Cp systems.

We used two different geometries for the metallocene fragment in $Cp_2Ti(CH_3)^+$: one based on Cp_2TiR_2 (this geometry was also used for the Cp_2TiH^+ system) and one based on a syndiospecific Zr catalyst that has the two ligands tied back with a CMe_2 link.[2h] The only difference in the geometries is that the first case has $\theta_{CpTiCp} = 132.6°$, whereas the second has $\theta = 118°$. In the first case we find the lowest energy methyl configuration has the methyl coplanar with the centroids and the metal,[22] but with a soft out-of-plane bending mode; the energy required to move the methyl 50° out of the plane is only 4.03 kcal/mol. In the second case, we find two minima, at w = 0° and 50°, of approximately equal

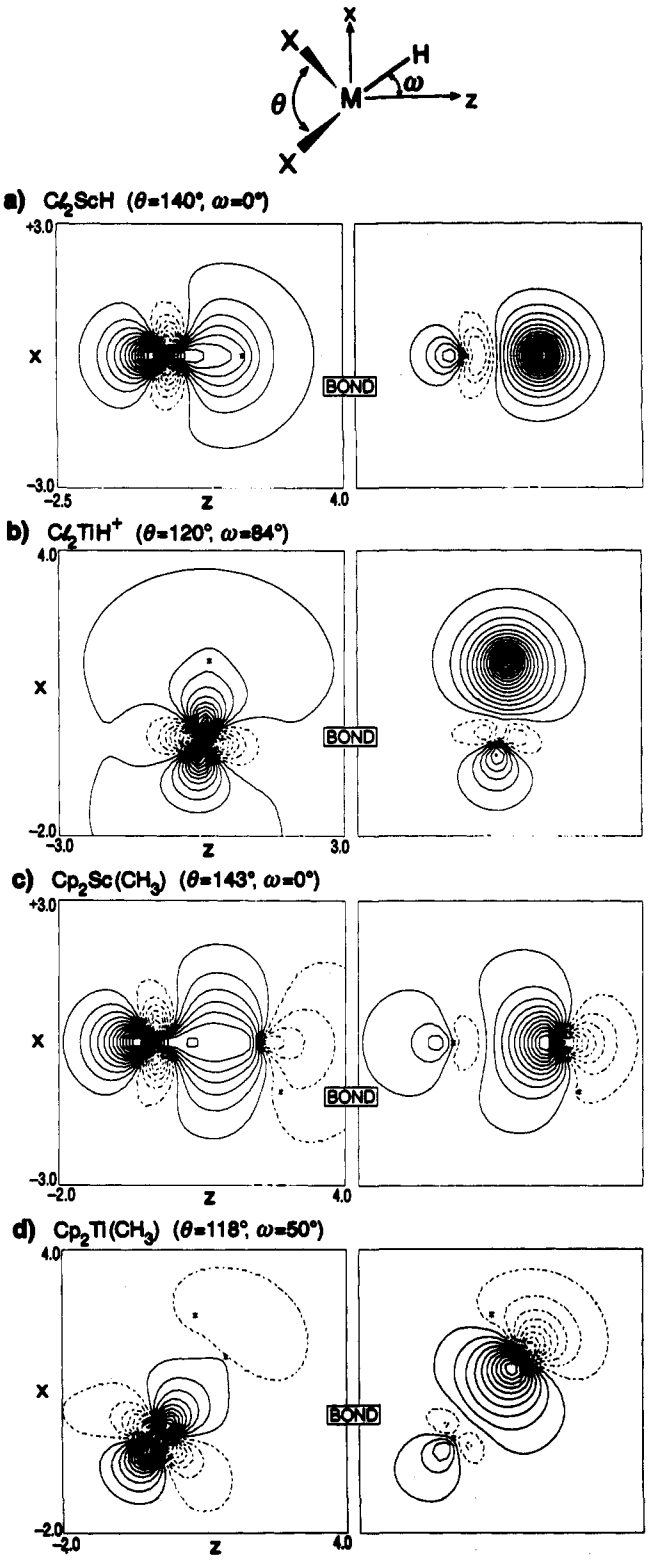

Figure 2. Bonding orbitals for Cl_2M–H: (a) Cl_2ScH, (ClScCl) = 180°, ω(plane–H) = 0°; (b) Cl_2TiH^+, θ(ClTiCl) = 120°, ω(plane – H) = 84°; (c) $Cp_2Sc(CH_3)$, θ(CpScCp) = 148°, ω(plane – CH_3) = 0°; and (d) $Cp_2Ti(CH_3)^+$, θ(CpTiCp) = 118°, ω(plane – CH_3) = 40°.

energy (within 1 kcal/mol), separated by a 6 kcal/mol barrier, and a third minimum 3 kcal/mol higher at about –30° with a 6 kcal/mol barrier.[23] These differences in the two metallocene fragments indicate that the decreased θ_{CpTiCp} (due to the link) improves the stereospecificity by stabilizing the out-of-plane structure.

Comparing the energy difference between ω = 0° and ω = 50° (ΔE) for the two comparable species X_2MR, M = Sc and Ti^+ [thus, giving a $\Delta\Delta E$], we find a consistent energy difference of 8–11 kcal/mol: 9.12 kcal/mol for Cl_2MH, 8.91 kcal/mol for $Cl_2M(CH_3)$, 8.58 for Cp_2MH, and 11.87 kcal/mol for $Cp_2M(CH_3)$ (for related metallocenes). Such a constancy in $\Delta\Delta E$ suggests that the differing electronic effects causing the $\Delta\Delta E$ in the scandium and titanium species are of a constant magnitude in all of the species, and that the variance in ΔE is due to steric effects. Thus, the $s^1d^2(Ti^+)$ has a 9.6 kcal/mol bias, favoring ω = 50°, rather than ω = 0°.

Similar $\Delta\Delta E$ can be used to extract differential steric interactions. Thus $\Delta\Delta E$ = 4.47 kcal/mol for Cl_2ScH to Cp_2ScH and $\Delta\Delta E$ = 4.01 kcal/mol for X_2TiH^+ suggests that the steric effects due to Cp···H are about 4.2 kcal/mol higher than for Cl···H. Similarly $\Delta\Delta E$ = 14.60 kcal/mol for X_2ScMe while $\Delta\Delta E$ = 11.64 kcal/mol for X_2TiMe^+ suggests that the steric factor due to Cp···CH_3 is about 13.1 kcal/mol higher than for Cl···CH_3.

III. Discussion

The above results show that group 4 cations have a strong bias for the alkyl or hydride ligand to move out of the plane described by the metal and other two ligands. In the case of the hydrides the preference is quite dramatic, while for the methyls the preference is tempered by electrostatic and steric repulsions. The group 3 catalysts, on the other hand, have no such bias; they are planar and require an additional 8–11 kcal/mol to become pyramidal (see Figures 3 and 4). Neutral group 4 species are also planar, requiring similar amounts of energy to become pyramidal.

To date, there has not been any *direct* experimental evidence for or against the nonplanar geometries we find for the group 4 cations. Some indirect evidence comes from experiments coupled with calculations on $[\eta^5\text{-}1,2\text{-}(CH_3)_2C_5H_3]ZrCH_3^+ \cdot CH_3B(C_6F_5)_3^-$, a well-defined cationic catalyst. From NMR studies, Yang *et al.*,[6b] find that the methyl resides out of the Cp–Zr–Cp plane, with a barrier to interchange between the methyl and the borate anion of 18.3 ± 0.2 kcal/mol at 80 °C. It must be kept in mind that this number includes the cation–anion interaction, which is the major component and difficult to separate from other effects. In an attempt to understand this exchange and determine the magnitude of the component effects, Castonguay and Rappé[17c] calculated the energy surface using molecular mechanics. In the presence of the counterion, they calculated the interchange barrier to be about 10 kcal/mol; in the absence of the counterion they found the barrier to be about 4 kcal/mol, so that the counterion accounts for 60% of the barrier. Taken together, these other results suggest that 7.3 of the 18.3 kcal/mol barrier is due to a nonplanar bias, in reasonable agreement with our value of about 6 kcal/mol for the Ti^+ species.

It is generally accepted that the group 4 cationic catalysts are far superior than group 3 catalysts in rates of turnover. Indeed Steigerwald and Goddard (SG)[19a] showed the related reaction $Cl_2MH + D_2 \rightarrow Cl_2MD + HD$ has a smaller barrier for Ti^+ than for Sc and Ti. SG showed that at the saddle point, the percent of d character in the M–H bond is 100% and hence that increased d character in the MH bonds leads to a lower barrier (Ti^+ has 84%, Sc has 63%, Ti has 72%). In addition, part of the superiority of group 4 cationic catalysts is due to the influence the ground-state geometry has on the energy of the transition state. For the group 3 catalysts, there is a significant reorganization energy associated with olefin complexation that would not be present in the group 4 cationic systems. Assuming that the intrinsic olefin binding energy is the same for both the scandium and titanium systems (most likely it would be stronger for Ti^+) and that binding requires a 50° out-of-plane angle, our results suggest that Ti^+

(22) No α-agostic stabilization was found for ground-state structures. To test this, we considered a fixed out-of-plane angle of 25°, and the methyl C_3 rotation axis was tilted 5° and 10° toward the Cp rings, relative to the bond vector. The relative energies are –0.096 and 0.256 kcal/mol, respectively.

(23) We define a positive angle (ω) by the methyl orientation that has the unique hydrogen pointing into the wedge.

Table 5. Energy Differences between 0° and 50° [c]

species	total energy, $\theta = 0°$ HF	GVB(1/2)	CI	CI + Q	total energy, $\theta = 50°$ CI + Q	$\Delta E\ E(50°) - E(0°)$
Cl_2ScH	-965.284 128 3	-956.306 194 9	-965.590 743 9	-965.617 754 0	-965.615 320 8	1.53
Cl_2TiH^+	-976.125 291 7	-976.181 955 4	-976.497 326 2	-976.535 263 3	-976.547 365 2	-7.59
Cl_2TiH	-976.537 760 1	-976.569 636 6	-976.857 544 5	-976.887 542 0	-976.884 818 5	1.71
$Cl_2Sc(CH_3)$	-1004.325 687 64	-1004.350 313 00	-1004.587 799 90	-1004.611 725 89	-1004.609 649 97	1.30
$Cl_2Ti(CH_3)^+$	-1015.197 889 50	-1015.254 880 13	-1015.530 567 53	-1015.566 846 01	-1015.578 977 87	-7.61
Cp_2ScH	-430.610 112 76	-430.627 638 82	-430.793 303 79	-430.813 763 94	-430.805 812 74	5.00
Cp_2TiH^+	-441.595 181 39	-441.633 061 48	-441.837 130 27	-441.869 753 76	-441.875 454 61	-3.58
$Cp_2Sc(CH_3)$	-469.634 834 6	-469.651 837 01	-469.878 890 82	-469.908 564 77	-469.883 228 15	15.90
$Cp_2Ti(CH_3)^+$ [a]	-480.621 375 55	-480.669 393 22	-480.931 867 34	-480.973 755 73	-480.967 328 96	4.03
$Cp_2Ti(CH_3)^+$ [b]	-480.565 831 49	-480.616 242 61	-480.874 220 62	-480.914 839 85	-480.914 025 13	0.511

[a] θ(CpTiCp) = 132.6. [b] θ(CpTiCp) = 118.0. [c] Chlorine systems include the core energy of chlorines, which is -889.423 72 Hartree. Total energies in Hartree, relative energy in kcal/mol.

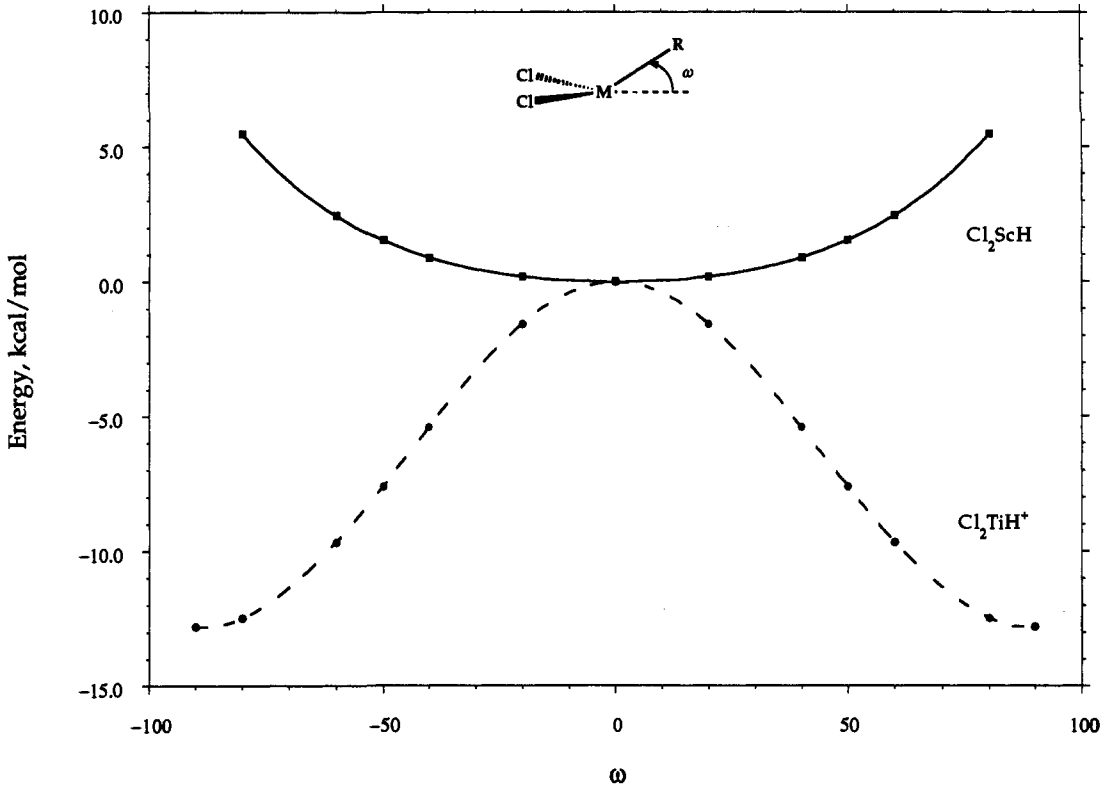

Figure 3. Energy as a function of angle from the plane, Cl_2MH.

has a 9–12 kcal/mol greater olefin binding energy[24] in the Cossee–Arlman mechanism.[13] Since the intrinsic binding of the olefin is greater for cationic than the neutral species, the preference of Ti^+ for the binding step is expected to be even greater. Previous theoretical results suggest that the intrinsic binding energy to $Cl_2Ti(CH_3)^+$ may be as large as 50 kcal/mol in the gas phase.[17a-c]

Most calculations on the transition state for ethylene insertion into a Ti–CH_3 bond have shown that the barrier is about 15 kcal/mol above the complexation step.[17] In solution there should be a barrier for the complexation step, due to displacement of weakly coordinated solvent molecules or counterions. Thus we suggest the solution phase energy profiles in Figure 5 for the reaction sequence. For scandium cases (Figure 5a) the insertion step is expected to be rate-determining since the complexation step would be endothermic (due to the large reorganization energy, small intrinsic binding energy, and energy required for solvent displacement). For Ti^+ the binding step should be exothermic (Figure 5b). This means that if the insertion barrier is small enough, the binding step may be rate-determining (Figure 5c), with a barrier due to solvent or counterion displacement. Currently the most widely accepted profile is that shown in Figure 5b, but 5c cannot be ruled out by current experiment results. These energy profiles are similar to those proposed previously for zirconocene reactions.[25]

Isotopic substitution experiments have been performed to test the importance of an α-agostic assisted mechanism in the insertion step, with differing results for the group 3 and group 4 systems.[26] In scandium systems a deuterium kinetic isotope effect (KIE) is observed, while for Ti^+ systems no such KIE is observed, and for Zr^+ a KIE is sometimes observed. The differences in the results can be rationalized using the above reasoning. Since the rate-determining step for the group 3 systems would be insertion, experiments would be expected to show a KIE for a mechanism involving α-agostic assistance for olefin insertion. If, on the other hand, olefin binding is rate-determining, as, for example, with an unhindered group 4 alkyl cation, little or no KIE would be observed, even if the (faster) olefin insertion step occurred with α-agostic assistance.

(24) We assume that the polymer must have a Ti–C angle of about 50° away from the plane in order to make room for the incoming monomer.

(25) Christ, C. S., Jr.; Eyler, J. R.; Richardson, D. E. *J. Am. Chem. Soc.* **1990**, *112*, 596.

(26) (a) Clawson, L.; Soto, J.; Buchwald, S. L.; Steigerwald, M.; Grubbs, R. H. *J. Am. Chem. Soc.* **1985**, *107*, 311. (b) Piers, W.; Bercaw, J. E. *J. Am. Chem. Soc.* **1990**, *112*, 9406. (c) Krauledat, H.; Brintzinger, H. H. *Angew. Chem., Int. Ed. Engl.* **1990**, *29*, 1412.

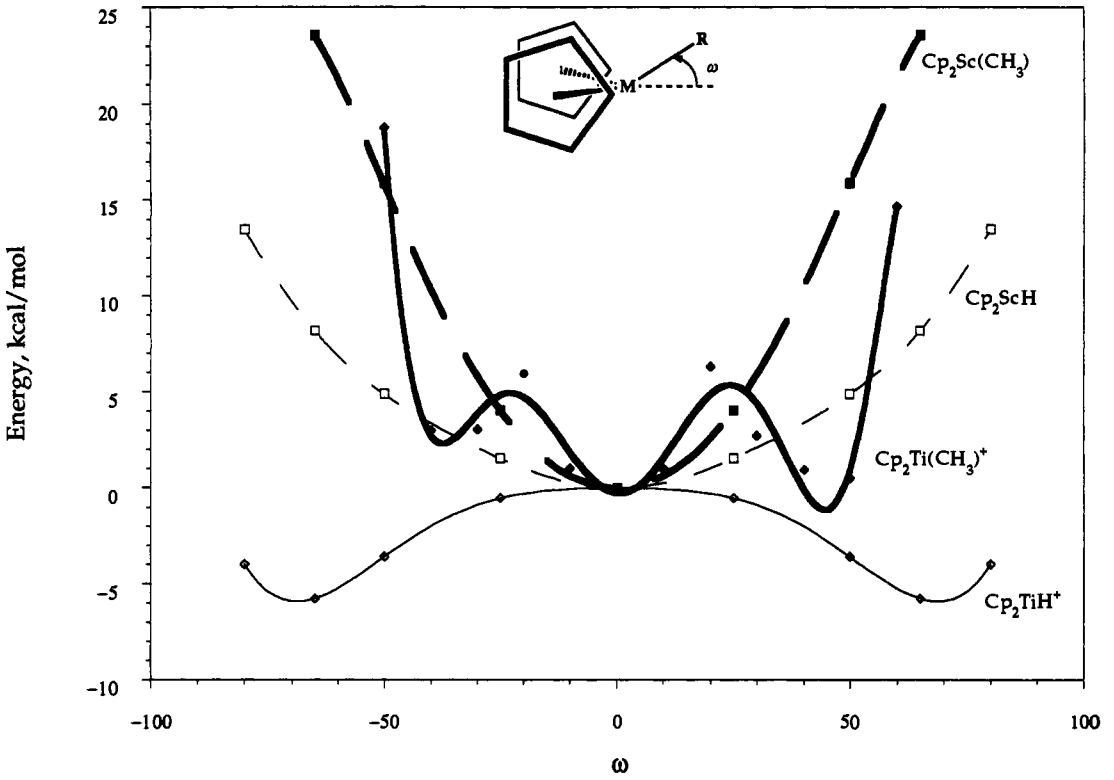

Figure 4. Energy as a function of angle from the plane Cp_2MR: (a) Cp_2MH and (b) $Cp_2M(CH_3)$.

The calculations for the neutral group 4 species suggest that Ti(III), Zr(III), and Hf(III) systems would have lower activity, due to the ground-state geometric effects described above. Indeed, the only insertion reactions found experimentally for Ti(III) systems are into the Ti–H bond of Cp_2*TiH and 2-butyne into Cp_2*Ti(CH_3).[27]

Recent mechanistic studies, both experimental and theoretical,[28] have attempted to understand the stereospecificity of homogeneous catalysts. It is recognized that the steric control of the ancillary ligands plays a major role in this stereospecificity, but the nature of chain control is still under debate. For isospecific catalysts, the nature of the chain control is not particularly crucial, as the ligands select the same prochiral face of the olefin, independent of the side to which the olefin binds. Thus, the position of the growing polymer chain is not a key element of the isospecific mechanism. However, as shown in Scheme 1, the chain's position is important for the syndiospecific catalysts, as the catalyst must regularly alternate between the two prochiral olefin faces (vide infra). Our results show that for group 4 cationic systems, the polymer chain prefers to remain off center following an insertion, which is consistent with previous calculations of the full reaction.[17a-c] Thus, the chain migration required by the Ewen *et al.* mechanism[10] is due to a ground-state electronic effect requiring the polymer chain to stay to the side following an insertion. Such a preference naturally leads to the chain migrating from side to side.

IV. Conclusions

In conclusion, we find that the group 4 cations have an inherent bias toward nonplanarity when bonded to two electronegative ancillary ligands such as Cp or Cl. The isoelectronic group 3 species have no such bias, nor do the group 4 neutrals. This difference is due to the different ground-state electronic configurations on the metals: the group 3 species are s^2d^1, while the group 4 cations are s^1d^2. When the ancillary ligands are Cp's bound to Ti^+ in the same geometry as in the Zr catalysts, we find three minima at −30°, 0°, and 50°, all separated by 6 kcal/mol barriers. We also find that the corresponding Sc species requires much more energy to move out-of-plane, the relative difference being about 12 kcal/mol for motion by 50°. As the methyl group is a good model for steric demands of the growing polymer chain, we expect that processes requiring the out-of-plane motion of the polymer, such as olefin binding, would be much more favorable (by about 12 kcal/mol) in the group 4 cation cases than in the group 3 cases. We also find a consistent energy difference between similar Sc and Ti^+ species for the $\Delta E(E(0°) = E(50°))$, suggesting that the electronic effects are of a constant magnitude for all systems.

These results are compatible with existing experimental evidence. The group 4 cations should have a stronger olefin binding and a lower overall barrier for chain propagation than the group 3 species, which they do, at least qualitatively. We also expect the group 4 neutrals to be poor catalysts, which they are. More importantly, the results shed light on some uncertainties concerning the Ziegler–Natta stereopolymerization mechanism. These results rationalize the apparent chain migration that is the key to the current explanation of the syndio-directing catalysts. We also speculate that the rate limiting step in the mechanism for the group 3 and group 4 species may be different, which could explain the different results in isotopic labelling experiments probing the transition state.

V. Calculational Details

All the metal–chlorine geometries reported were calculated using generalized valence bond (GVB) wave functions with the perfect pairing restriction (GVB-PP) for a single valence bond structure.[15] The calculations were carried out using both the GVB suite of programs[29] and the MOLECULE-SWEDEN suite.[30] Generally only the M–R bond was correlated [GVB-(1/2)], and the geometry optimizations were performed using standard gradient methods. Using the GVB orbitals, we included

(27) Luinstra, G. A. Thesis Rijksuniversiteit Groningen, 1991; p 30.
(28) (a) Venditto, V.; Guerra, G.; Corradini, P.; Fusco, R. *Polymer* **1990**, *31*, 530. (b) Cavallo, L.; Corradini, P.; Guerra, G.; Vacatello, M. *Polymer* **1991**, *32*, 1329.

(29) The GVB suite of programs, written at Caltech under the supervision of Goddard, W. A., III, *et al.*, Caltech, unpublished.

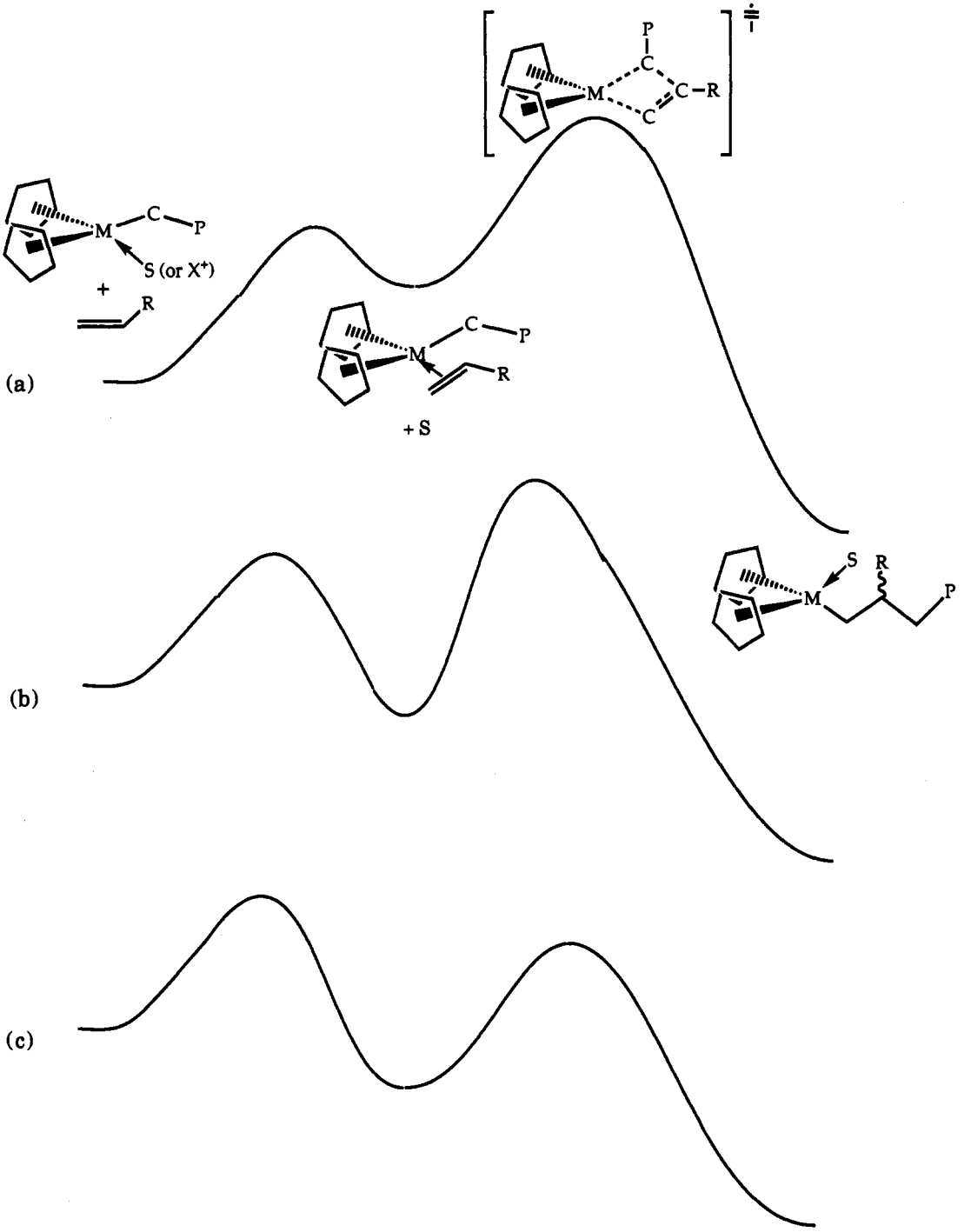

Figure 5. Solution-phase energy profiles for (a) endothermic olefin binding, rate-determining insertion step, (b) exothermic olefin binding, rate-determining insertion step, and (c) exothermic olefin binding, rate-determining binding step.

additional electron correlation as follows: For the metal–chloride systems we allowed all single and double excitations from the GVB(1/2) wave functions (two configurations) to all virtual orbitals, denoted as GVB*SD. For the metal–Cp systems, this GVB*SD calculation was not practical, and a restricted set of excitations was utilized. For accurate energies, it is imperative that the metal be described as well as possible, so a CI wave function was calculated using the two GVB-PP configurations as references but restricting excitations to the M–C (or M–H) bond, the six π orbitals on the Cp's and the three valence orbitals on the alkyl group. This wave function, denoted as GVB*CpCI, should adequately describe the metal–Cp interactions in addition to the metal–alkyl interactions. All energies reported include the Davidson correction.

Effective core potentials (ECP's) were utilized to describe the core electrons for the metals, chlorine, and silicon.[16] These ECPs were derived from all electron atomic interactions but treat explicitly only the valence electrons. For chlorine and silicon the Ne core is replaced so that there are seven and four valence electrons, respectively, where the basis sets and ECP's are from Rappé, Smedley, and Goddard.[16c] For Sc and Ti, the outer core electrons (3s and 3p) were included explicitly along with the 3d, 4s, and 4p valence electrons. Thus, for Sc and Ti^+ we treated 8 + 3 = 11 electrons explicitly (12 electrons for Ti). For the geometry optimizations, the metal basis sets and ECP's used were

(30) MOLECULE-SWEDEN is an electronic structure program system written by J. Almlöf, C. W. Bauschlicher, M. R. A. Blomberg, D. P. Chong, A. Heiberg, S. R. Langhoff, P.-A. Malmqvist, A. P. Rendell, B. O. Roos, P. E. M. Siegbahn, and P. R. Taylor.

Table 6. Recontracted Hay-Wadt Basis Sets[a] for Group 4 Cations

	Ti^+	
	ζ	c
ns	4.3720	−0.3667
	1.098	0.8360
	0.4178	0.4025
$(n+1)s$	1.0980	−0.0603
	0.4178	−0.2949
	0.1452	0.5837
	0.0523	1.000
np	12.52	−0.463
	1.491	0.6346
	0.4859	0.4598
$(n+1)p$	0.0530	1.000
	0.016	1.000
nd	20.2100	0.0287
	5.495	0.1433
	1.699	0.3706
	0.484	0.4739
	0.1157	1.000

[a] See ref 16d.

Table 7. Basis Sets Developed for the Hurley *et al.* ECPs[a,b]

	Sc		Ti^+	
	ζ	c	ζ	c
ns	11.12	0.01680	12.40	−0.175
	4.205	−0.37353	4.7170	0.3863
	1.169	0.62961	1.340	−0.6408
	0.431	0.60351	0.4880	−0.6040
$(n+1)s$	4.205	0.05078	4.7270	−0.0607
	1.169	−0.12935	1.340	0.1574
	0.431	−0.27675	0.4880	0.3321
	0.0825	0.54725	0.10723	−0.8070
	0.03376	1.000	0.04483	1.000
np	1.494	0.473	1.7110	0.4719
	0.4602	0.622	0.5256	0.6256
$(n+1)p$	0.08925	1.000	0.10723	1.000
	0.03376	1.000	0.04483	1.000
nd	15.132864	0.0390	20.210	0.0343
	4.204818	0.1779	5.4950	1.711
	1.303034	0.4429	1.6990	0.4456
	0.368257	1.000	0.4840	0.5422
	0.081226	1.000	0.1157	1.000

[a] See ref 16e. [b] See ref 31.

those developed by Hay and Wadt,[16d] but with the basis sets recontracted for the cations. For energetic calculations, a modified set, derived from the FOURS basis set of Rappé and Goddard,[31] was used in conjunction with the ECP's developed by Hurley *et al.*[16e] For all the carbon atoms we used the Dunning–Huzinaga double-ζ basis (9s5p/3s2p) and included polarization functions ($\zeta = 0.75$) for the $Cl_2M(CH_3)$ systems. The hydrogen basis set was the unscaled set of Dunning and Huzinaga (5s/3s) if bonded directly to the metal, otherwise it was the scaled set (4s/2s) ($\zeta = 1.2$). Tables 6 and 7 contain all sets that were modified.

In performing the geometric calculations on the metallocenes, the M–R distance was optimized. The rings were fixed such that the metallocene fragment would have a symmetry plane relating the two rings, and that the unique apex of each ring points toward the alkyl group. The C–C and C–H bond lengths in the rings were 1.40 and 1.08 Å, respectively. The metal–centroid geometries are in Table 1. In addition, the methyl groups were frozen in reasonable geometries, based on the optimized geometries of $Cl_2M(CH_3)$, which are given with Table 1.

(31) Rappé, A. K.; Goddard, W. A., III *The FOURS Basis*; unpublished.

Acknowledgment. We wish to thank Dr. Jason Perry for many helpful discussions. E.P.B. wishes to acknowledge a generous grant from the ARCS foundation. This research was supported by a grant from the National Science Foundation (CH 91-100284) and the USDOE Office of Basic Energy Sciences (Grant No. DE-FG03-85ER113431). The facilities of the Materials and Molecular Simulation Center are also supported by grants from NSF-GCAG, DOE-AICD, Allied-Signal, Asahi Glass, Asahi Chemical, BP America, Chevron, BF Goodrich, Teijin Chemical, and Xerox.